

UC Irvine

UC Irvine Previously Published Works

Title

Photon-density wave fluctuation correlation spectroscopy: study of coherence in the brain and muscles

Permalink

<https://escholarship.org/uc/item/8c31s87t>

Authors

Toronov, Vlad
Filiaci, Mattia A
Franceschini, Maria-Angela
[et al.](#)

Publication Date

1999-07-15

DOI

10.1117/12.356814

Copyright Information

This work is made available under the terms of a Creative Commons Attribution License, available at <https://creativecommons.org/licenses/by/4.0/>

Peer reviewed

Photon-density-wave fluctuation-correlation-spectroscopy: study of coherence in the brain and muscles

Vlad Toronov, Mattia Filiaci, Maria Angela Franceschini, Sergio Fantini, and Enrico Gratton

Laboratory for Fluorescence Dynamics, Department of Physics,
University of Illinois at Urbana-Champaign

ABSTRACT

Using photon-density-wave fluctuation-correlation-spectroscopy, we studied the fluctuations of the optical signal measured in the brain and skeletal muscles. We investigated the autocorrelation power spectra at specific tissue locations, and the coherence between different tissue regions in the frequency band 0-0.3 Hz. We found specific dominant frequency components that can be assigned to vasoconstriction activity. In a measurement protocol involving voluntary motor stimulation (right hand finger movements), we found that the optical fluctuations observed in the left forearm muscle and in the left cerebral motor cortex show different coherence features at rest and during stimulation. These changes are particularly significant at the frequencies associated with vasoconstriction activity. A power-spectrum analysis of the optical fluctuations revealed a resonance-like dependence of the optical signal at the motor cortex on the period of the motor stimulation sequence.

Keywords: Photon density waves, fluctuations, power spectrum, coherence, synchronization, vasoconstriction activity

1. INTRODUCTION

Photon-density-wave near-infrared (NIR) spectroscopy is a useful method for the non-invasive study of hemodynamic changes in tissue optical properties over time scales ranging from milliseconds to hundreds of seconds. Recently, NIR was applied to studies of brain processes, particularly changes of oxy- and deoxy- hemoglobin concentrations ([HbO₂] and [Hb], respectively) induced by motor or visual stimulation (see Ref.1 for a review of these studies). Most groups reported an increase of [HbO₂] and total blood volume and a simultaneous monotonic decrease of [Hb] during stimulation.¹ However some researchers observed a stimulus-induced increase of both [HbO₂] and [Hb].² Another open question is the spatial localization of the cerebral area exhibiting an optical response to stimulation: some groups reported that only localized areas were excited,^{3,4} but others observed dynamic responses of [HbO₂] in the entire area of measurement.⁵

Usually, signals acquired on the human head reflect complex time changes of tissue optical properties and require statistical methods to be interpreted. The most popular method is the folding average of the signals over a number of cycles of repetitive stimulations. However, this approach is effective only in the case of a significant phase synchronization of the optical signal with the stimulation sequence. Although such a synchronization is usually implicitly assumed, it may not always occur. We present a NIR study of motor cortex responses to periodic stimulations by means of fluctuation correlation spectroscopy. We use this method not only to assess the dynamics of the optical signal at the motor cortex, but also to analyze its coherence with the signals collected at other tissues such as the forearm muscle and the superficial scalp-skull layers.

2. INSTRUMENTATION AND METHOD

For the measurements on the head, we use a two-wavelength instrument in which NIR light emitted by laser diodes (758 and 830 nm) is guided to the tissue through multi-mode silica optical fibers. Up to 16 diodes can be used in a sequential multiplexing mode. Two glass fiber bundles collect the scattered light and conduct it to the photomultiplier tube detectors. The 16 sources and 2 detectors provide 32 possible source-detector combinations. An additional instrument with a one-

source/one-detector probe (830 nm wavelength, 2 cm source-detector distance) is used to acquire the signal on the left forearm muscle. The signals from the three PMTs are applied to the inputs of an interface card for an IBM-PC computer, where data processing is performed.

The time series of the intensity values are processed to calculate the autocorrelation power spectra, cross-correlation coherence for different signals, and the temporal changes in [HbO₂] and [Hb]. The spectra are obtained by averaging the Fourier-transforms of consecutive subsets of the data series. The bandwidth and the frequency resolution of the auto- and cross-correlation spectra are determined by the sampling rate and the length of the time series subset. For the measurements reported in this work the acquisition time per point is 160 ms, which corresponds to a frequency bandwidth of 3.125 Hz. The duration of each subset data trace to produce a Fourier- transform is 164 s, which corresponds to a spectral resolution of 0.0061 Hz.

To convert light intensity data into hemodynamic parameters, we assume a model in which the absorption of light in the tissue is provided only by oxy- and deoxy-hemoglobin.⁶ This model gives the following equations to compute the changes of [HbO₂] and [Hb] corresponding to the changes of the light intensities $I_{\lambda 1}$ and $I_{\lambda 2}$ from their initial values $I_{0\lambda 1}$ and $I_{0\lambda 2}$:

$$\Delta[HbO_2] = \frac{\Delta\mu_a^{\lambda 1} \epsilon_{Hb}^{\lambda 2} - \Delta\mu_a^{\lambda 2} \epsilon_{Hb}^{\lambda 1}}{\epsilon_{HbO_2}^{\lambda 1} \epsilon_{Hb}^{\lambda 2} - \epsilon_{Hb}^{\lambda 1} \epsilon_{HbO_2}^{\lambda 2}}, \quad 1(a)$$

$$\Delta[Hb] = \frac{\Delta\mu_a^{\lambda 2} \epsilon_{HbO_2}^{\lambda 1} - \Delta\mu_a^{\lambda 1} \epsilon_{HbO_2}^{\lambda 2}}{\epsilon_{HbO_2}^{\lambda 1} \epsilon_{Hb}^{\lambda 2} - \epsilon_{Hb}^{\lambda 1} \epsilon_{HbO_2}^{\lambda 2}}, \quad 1(b)$$

$$\Delta\mu_a^\lambda = -\frac{\ln(I_\lambda / I_{\lambda 0})}{d\sigma_\lambda}. \quad 1(c)$$

Here $\epsilon_{Hb}^{\lambda 1,2}$ and $\epsilon_{HbO_2}^{\lambda 1,2}$ are the extinction coefficients of Hb and HbO₂, respectively, at the wavelengths $\lambda 1$ and $\lambda 2$, $\Delta\mu_a^\lambda$ is the change in the absorption coefficient of the tissue at the wavelength λ , d is the distance between the source and the detector fibers, and σ_λ are the adult head differential path-length factor (DPF) values, taken equal to 6.2 at $\lambda=758$ nm and 5.9 at $\lambda=830$ nm according to Ref. 7.

For measurements on the human head we designed a headset consisting of the fiber-optic probe shown in Fig.1 and a frame securing the probe on the head. Two detector fibers are securely fixed in the central part of the probe (see Fig.1 for distances). The paired (758 and 830 nm wavelength) source optodes are attached to the probe pad at 8 positions. The range of source-detector distances allows us to distinguish processes occurring at different tissue depths.

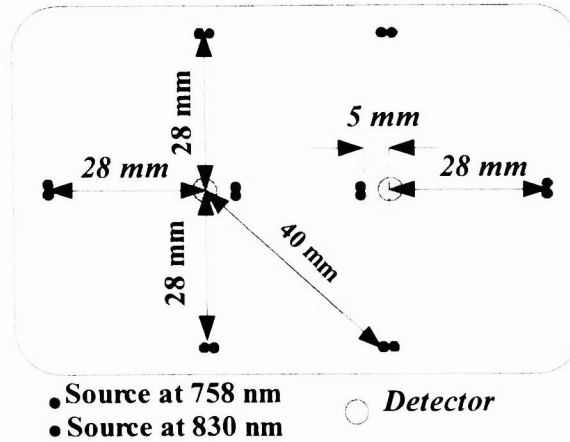


Fig. 1. Geometric arrangement of the optical fibers in the probe designed for measurements on the head.

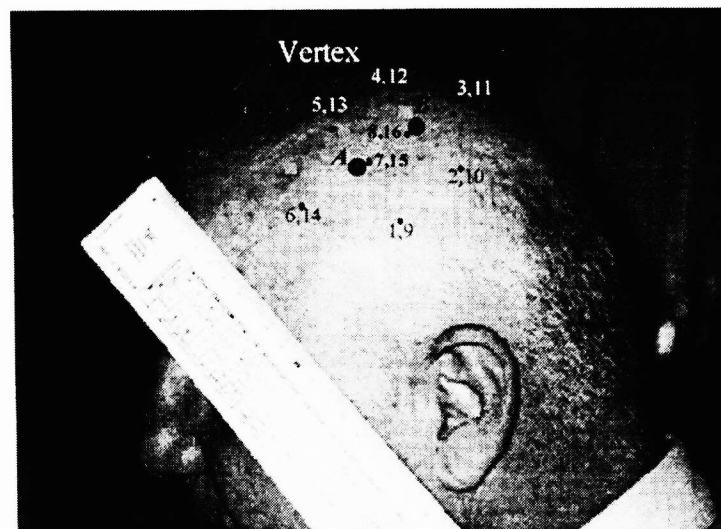


Fig.2. Locations of the source and detector fibers on the head. Sources 1-8 emit light at 758 nm, sources 9-16 – at 830 nm. The detector A is placed in the area of the primary motor cortex.

We performed measurements on 5 subjects, right-handed males of age ranging from 30 to 65 years. A written informed consent was obtained from each subject before measurements. Figure 2 shows the locations of the source and detector fibers on a subject's head. The probe is installed on the left part of the head in such a way that the detector A is in the area of the primary motor cortex. The one-source probe is attached to the left forearm muscle of the subject. During measurements the subjects are comfortably supine and instructed not to speak or to make unnecessary movements. Each measurement consists of a 10 min rest epoch and a 20-40 min exercise epoch consisting of a certain number of exercise/rest cycles. During rest the base-line data is acquired and the breathing rate is estimated by counting the number of breaths per three minutes. During the exercise, subjects are asked to begin or stop performing a finger-motion (palm squeezing) exercise. Only the right hand is exercising for each measurement, and the squeezing rhythm (1.5 Hz) is maintained by means of a metronome. During the exercise epoch subjects perform 4 exercise series differing by the duration of the stimulation/relaxation period: 20/60 sec, 20/20 sec, 10/17 sec, and 10/10 sec, and consisting of 10 periods each.

3. RESULTS

A sample of hemoglobin changes in the head and of DC signals in the non-exercising (left) forearm is represented in Figures 3 and 4 respectively (the signals were low-pass filtered to remove the arterial pulse oscillations). The stimulation periods are shown by gray bars in both figures. As Fig.3 shows, under rest conditions [HbO₂] and [Hb] exhibit spontaneous fluctuations of approximately the same amplitude both at the motor cortex (channel (5,13 A)) and at a distance of about 4 cm to (see Fig. 2) from the motor cortex (channel (3,11 B)). During Exercise 2 (10/17 sec stimulation/relaxation period) one can see regular changes of [HbO₂] and [Hb] in channel (5,13 A) (motor cortex). Particularly, the [Hb] and [HbO₂] oscillations are synchronous with the stimulation sequence. These hemoglobin concentration changes are in agreement with the pattern obtained by most researchers by folding average analysis: during the stimulation [HbO₂] increases and [Hb] decreases, while during the relaxation the directions of changes are opposite. Furthermore, in exercise 2, almost no activity is observed in channel (3,11 B), indicating a spatial localization of the activity. During Exercise 1 (20/20 sec stimulation/relaxation period) the character of the hemoglobin concentration traces is intermediate between the rest and Exercise 2 conditions. In channel (5,13 A) (motor cortex) one can recognize a pattern which correlates with the stimulation sequence, but its periodicity is significantly less regular than for the Exercise 2. Furthermore, the signal in channel (3,11 B) does not show any synchronization with the stimulation, but it rather undergoes some irregular changes.

Figure 4 reveals a prominent periodic pattern in the DC signal from the non-exercising forearm both under exercise and rest conditions. We found that the frequency of this periodic pattern corresponds to the breathing rate. We believe that the physiological origin of these oscillations is the modulation of the vasoconstriction activity at the breathing frequency, also known as Traube-Hering wave.⁸ In fact, we observed this modulated pattern also in the absorption coefficient measured by the multi-distance technique, implying that it is unlikely due to the motion effects. This pattern is more regular in the case of Exercise 2, which also shows an average oscillation amplitude approximately twice as high than at rest and Exercise 1 conditions. Note that all of the data shown in Figs. 3 and 4 were obtained from the same subject during the same sequence of measurements.

Figure 5 represents the normalized power spectra and the coherence of the intensities at 830 nm measured in the channel (13 A) (motor cortex, see Fig.2) and in the non-exercising (left) forearm. The subject and conditions (rest, Exercises 1 and 2) are the same as in Figs. 3 and 4. The bottom triangular markers show the harmonics of the Exercise 1 frequency, while the top markers show the harmonics of the Exercise 2 frequency. The letter "T" indicates the frequency of Traube-Hering wave, which was measured during the experiment by counting the number of breaths per minute. One can see that at rest, the maximum peak of the head signal power spectrum in the range of 0.1-0.3 Hz (shown by letter "M") occurs at a lower frequency than the Traube-Hering wave. (The vasoconstriction oscillations at a frequency lower than the respiratory rate are known as Mayer waves.⁸) The coherence spectrum of the head and forearm signals at rest reaches its highest values at the respiratory frequency and its right side-band, possibly generated by the interaction of Mayer and Traube waves.

During Exercise 1 the structure of the non-exercising forearm power spectrum signal is qualitatively the same as at rest. In the head signal spectrum, a new small peak appears at the frequency of the stimulation sequence (Exercise 1 in the Fig.5), the Mayer wave frequency slightly moves to the left (towards the nearest harmonic of the stimulation frequency), while the respiratory peak and its side-band are suppressed. The coherence at Mayer wave frequency is significantly higher than at rest, but still the maximum of coherence is at the respiratory frequency (T).

The most evident changes from the rest power spectra occur at Exercise 2. The peak at the exercise frequency in the power spectrum of the head signal (Exercise 2 in Fig.5) is more pronounced than in the case of Exercise 1. Furthermore, the Traube-Hering and Mayer waves lock on the same frequency at which both forearm and head spectra obtain prominent peaks. Note that the frequency of this peak coincides with the frequency of the fourth harmonic of the exercise. We also observe that this harmonic frequency almost exactly coincides with the Mayer wave frequency recorded under rest conditions. In the coherence spectrum, there are prominent peaks at the second and fourth harmonics of the Exercise 2 frequency.

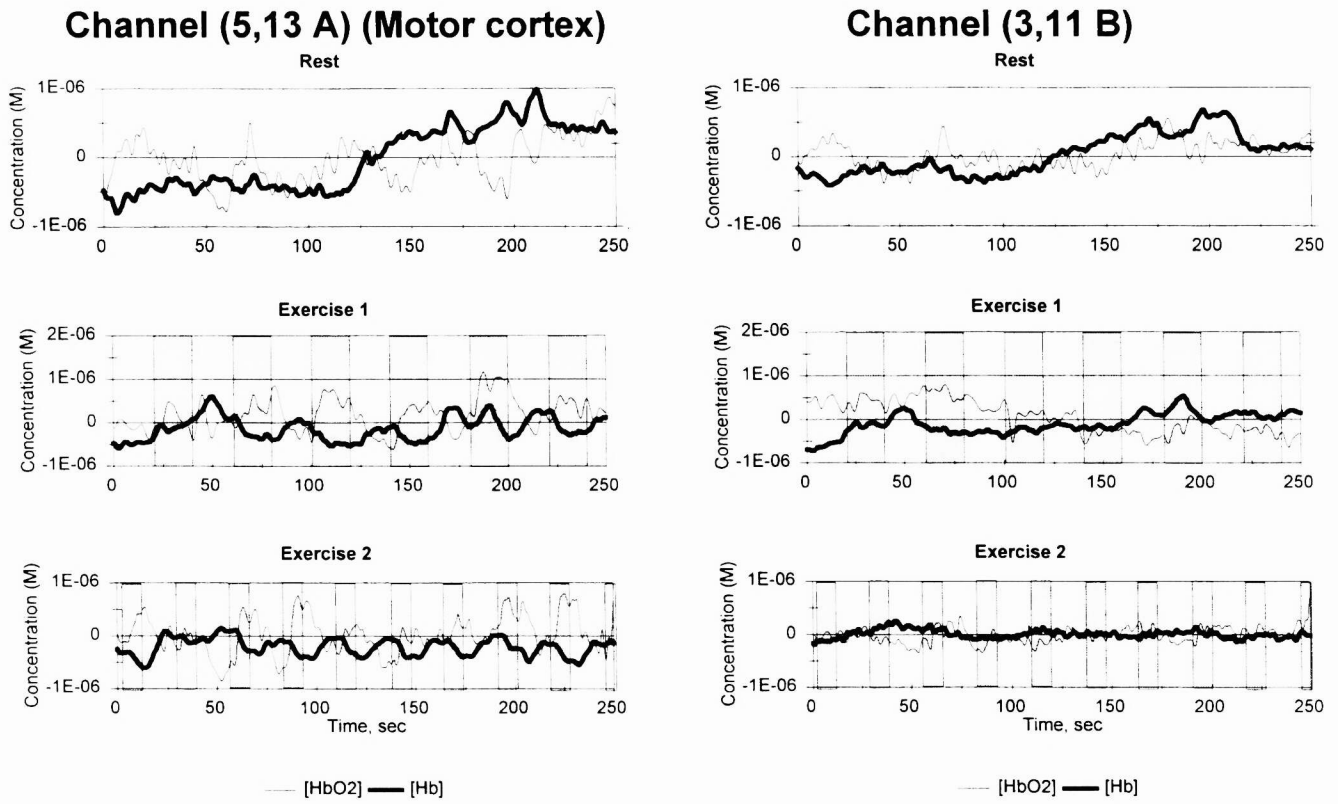


Fig.3. Hemoglobin concentration changes measured in the head at two different locations (see Fig. 2 for channel positions) during the rest and exercise protocols 1 and 2. Gray bars indicate the periods of finger movements.

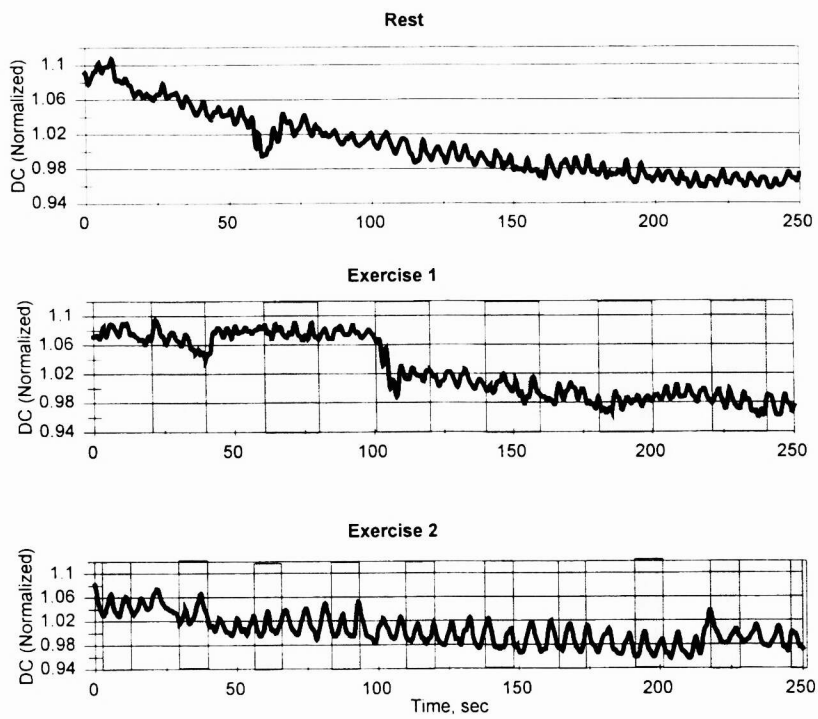


Fig.4. Intensity at 830 nm measured in the non-exercising (left) forearm. Gray bars indicate the periods of the right-hand finger movements.

Normalized Power Spectra

Coherence

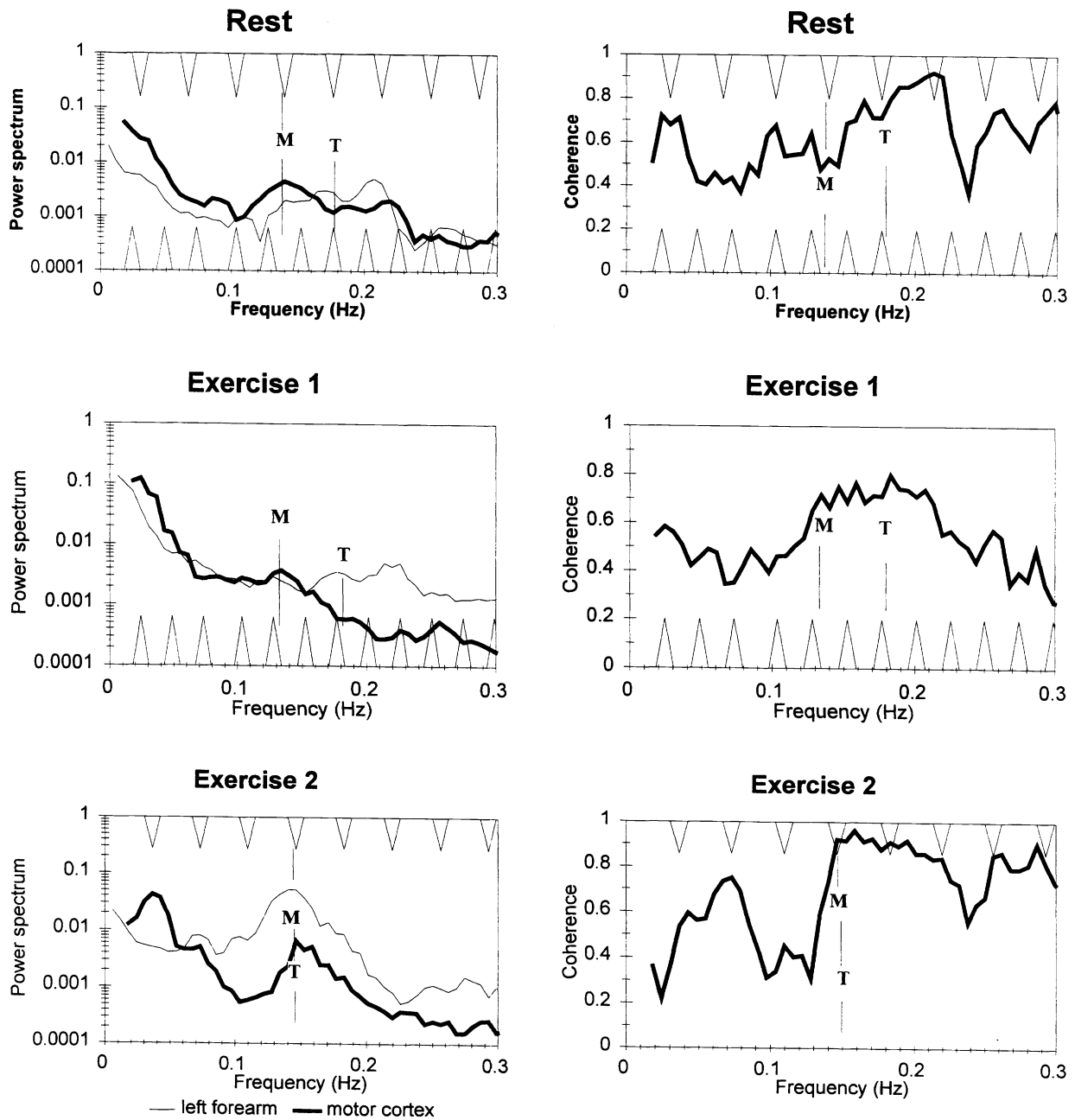


Fig.5 Power and coherence spectra of the intensity at 830 nm acquired on the motor cortex and on the left (non-exercising) forearm during the rest and exercise protocols 1 and 2. The letter T indicates the frequency of the Troube-Hering wave, while the letter M shows the frequency of the Mayer wave.

In most cases the signals in the short-distance (0.5 cm) channels ((7,8 A) and (15,16 B) in Fig. 2) are not synchronized with the exercise sequence. However, in a few cases of resonance we did observe short-distance signals synchronous with the exercise sequence. In these cases, however, the average ratio of the change in [Hb] to the change in [HbO₂] was 4-5 times smaller than the ratio calculated from large-distance signals.

4. DISCUSSION AND CONCLUSION

Our results show that for specific frequencies of the stimulation/relaxation sequence one can observe [HbO₂] and [Hb] changes that are spatially localized and synchronous with the stimulation sequence. Such a synchronization occurs when the stimulation sequence frequency or one of its harmonics nearly coincides with the major power spectrum peak in the band of 0.1-0.3 Hz (Mayer waves) preexisting in the brain fluctuations at rest. Respiratory frequency also locks to the Mayer wave frequency at resonance. When synchronized, hemoglobin saturation changes in agreement with the typical pattern: during the stimulation [HbO₂] increases and [Hb] decreases, and during the relaxation the directions of changes are opposite. In most subjects, there is a tendency to exhibit larger hemoglobin response in that part of the measured area which is close to the motor cortex. Superficial head tissue can exhibit significant oxy-hemoglobin changes synchronous with stimulation. We would like to underline that the clear spatially localized and synchronized with sequence pattern of the hemoglobin changes appears only at specific stimulation frequencies. In most cases, we did not observe synchronization at first, but it appeared when the stimulation period was changed. This result is consistent with the observation by Obrig et al.⁹ that at the given duration of the stimulation, a significant hemoglobin response occurs at a specific length of the interstimulus interval.

The observed features of resonance synchronization suggest that the hemoglobin waves induced by the brain stimulation interact with the preexisting Mayer and Traube-Hering waves of vasoconstriction activity. If such an interaction exists, it apparently has a complex, possibly nonlinear nature. It may result both in complex non-periodic changes of [HbO₂] and [Hb] under some exercise conditions, and in a regular behavior at others.

Whether or not synchronization occurs, the coherence spectrum of fluctuations in the brain and forearm reaches its highest value at the respiratory frequency. The coherence of vasoconstriction fluctuations at the respiratory frequency in different parts of the body shows the global nature of these fluctuations. Together with the resonance locking of the Traube-Hering and Mayer waves to the harmonic of the stimulation frequency, this can explain the synchronous (with the stimulation) changes of blood flow in the superficial head tissues, if one assume a nonlinear interaction between the vasoconstriction waves and the hemoglobin response to the repetitive stimulation.

To conclude, we have studied the power spectra and the coherence of near-infrared signals in the motor cortex, forearm muscle and superficial head tissues under rest conditions and during repetitive motor stimulations. Our results indicate a complex resonance-like interaction between the hemodynamics induced by the sequence of stimulations, and preexisting vasoconstriction oscillations. Under resonance conditions, this interaction results in hemoglobin concentration changes that are spatially localized and synchronous with the stimulation sequence, but complex spatial-temporal patterns may occur off resonance.

ACKNOWLEDGMENTS

This work was supported by National Institutes of Health (NIH) Grant CA57032, and Whitaker-NIH Grant RR10966.

REFERENCES

1. A. Villringer and B. Chance, "Non-invasive optical spectroscopy and imaging of human brain function", *TINS* **20**, pp. 435-442, 1997
2. T. Kato, A. Kamei, S. Takashima, and T. Ozaki, "Human visual cortical function during photic stimulation monitoring by means of near-infrared spectroscopy", *J. Cereb. Blood Flow Metab.* **13**, pp.516-520, 1993.

3. A. Kleinschmidt, H. Obrig, M. Requardt, K.D.Merboldt, U Dirnagl, A. Villringer, and J.Frahm, "Simultaneous recording of cerebral blood oxygenation changes during human brain activation by magnetic resonance imaging and near-infrared spectroscopy", *J. Cereb. Blood Flow Metab.* **16**, pp. 817-826, 1996
4. B. Chance, Q. Luo, S. Nioka, D.C. Alsop and J.A. Detre, "Optical investigations of physiology: a study of biomedical contrast: intrinsic and extrinsic", *Proc. R. Soc. London B Biol. Sci.* **352**, pp. 707-716, 1997
5. A. Maki, Y. Yamashita, Y. Ito, E. Watanabe, Y. Mayanagi, and H. Koizumi, "Spatial and temporal analysis of human motor activity using noninvasive NIR topography", *Med. Phys.* **22**, pp. 1997-2005, 1995
6. S. Fantini et al., "Frequency-domain multichannel optical detector for noninvasive tissue spectroscopy and oximetry", *Optical Engineering*, **34**, pp. 32-42, 1995
7. A. Duncan et al., "Optical pathlength measurements on adult head, calf and forearm and the head of the newborn infant using phase resolved optical spectroscopy", *Phys. Med. Biol.* **40**, pp. 295-304, 1995
8. R. M. Berne and M. N.Levy Eds ,*Physiology*, Third Edition, Mosby Year Book, St. Louis 1990, p.485
9. H. Obrig, C. Hirth, J.G. Junge-Hulsing, C. Doge, R. Wenzel, T. Wolf, U. Dirnagl, and A. Villringer, in *Oxygen Transport to Tissue XVIII*, edited by Nemoto and LaManna, Plenum Press, New York, 1997, pp.471-481